EXECUTIVE SUMMARY OF THE THESIS

Continuum approach for fragmentation event modelling and breakup severity assessment in Low Earth Orbit

LAUREA MAGISTRALE IN SPACE ENGINEERING - INGEGNERIA SPAZIALE

Author: FRANCESCA OTTOBONI

Advisor: PROF. CAMILLA COLOMBO

Co-advisor: LORENZO GIUDICI, MARTINA RUSCONI

Academic year: 2022-2023

1. Introduction

The sustainability of the space environment around the Earth is becoming an increasingly important research topic in the space sector. Past space missions have left a large number of inoperative objects in orbit. Despite the adopted mitigation measures, these objects contribute to the space debris population and its exponential growth, posing an increasing risk to operational satellites, and potentially leading to a collisional cascading effect known as *Kessler syndrome*.

Several methods have been developed throughout the years to model debris. The semi-deterministic approach requires the propagation of the trajectory of individual fragments, making the analysis computationally expensive. Instead, the probabilistic approach stems from the idea of considering the debris cloud as a whole. Some of these models treat the debris population as a fluid with continuous properties. Modelling debris clouds by means of their spatial density allows to significantly reduce the computational cost of the analysis.

In this work, a continuum approach is used to study the debris clouds generated in fragmentation events in Low Earth Orbit (LEO). The evolution of the clouds under the effect of drag is described through the spatial density with the continuity equation. An analysis on the optimal definition of area-to-mass ratio bins for the fragments is carried out, evaluating a further definition with respect to previous works [6]. Then, the collision probability of target spacecraft with the fragments is assessed in analogy with gas kinetic theory, correcting the model previously implemented in [7]. The model is applied to evaluate the severity of breakups occurring at various altitudes and inclinations with respect to representative targets spacecraft at different epochs, producing *effect* maps. A novel approach is introduced for the generation of the maps, i.e. the evaluation of the collision probability at variable time steps taking into account the lifetime of debris clouds.

2. Continuum formulation

A continuum model is developed in the first part of this work, using as reference the model of Letizia et al. [6]. The debris cloud generated by either a collision or an explosion is studied through four main blocks:

- A breakup model to characterise the fragmentation.

- Numerical propagation of the Keplerian elements of the fragments, until the continuum formulation can be applied.
- Spatial density function, translating the orbital parameters of the fragments into a continuous function depending on altitude and latitude.
- Continuum propagation of the spatial density.

2.1.   Breakup model

The adopted breakup model is the NASA Standard Breakup Model [3], which is a semi-empirical model able to simulate the characteristics of the fragments generated in a breakup, given some initial conditions. The model defines the number, the size, the area-to-mass (A/M) ratio and the ejection velocity of the generated fragments. These parameters are not constant for all debris, as they follow a distribution in characteristic length, which is taken as the independent variable to compute the characteristics for each fragment. This implementation of the breakup model can produce three kinds of fragmentation events: catastrophic collisions, non-catastrophic collisions and explosions.

2.2.   Numerical propagation

After the fragmentation, the debris cloud evolves under the effect of atmospheric drag and the Earth's oblateness. Initially, the fragments form an ellipsoidal cloud centred at the location of the breakup. In the second phase of the evolution, the cloud is stretched along the orbit of the parent spacecraft forming a torus around the Earth [10]. The torus is then gradually dismantled in phase three, due to the different variations of right ascension of the ascending node (Ω) and argument of pericentre (ω) of each fragment caused by Earth's oblateness [10]. As a result, the debris cloud forms a band around the Earth. At this point, ω, Ω and the mean anomaly $\overline{M}$[1] are randomised and drag can be considered as the dominant perturbation, hence the continuum formulation becomes applicable. The band formation time is estimated *a priori* based on the knowledge of the initial orbit. The orbital parameters of the fragments are propagated with the Gauss' equations until band for-

---

[1]The notation $\overline{M}$ is introduced to avoid confusion with the mass M.

mation. The effect of aerodynamic drag is evaluated by using an exponential model for the density. The secular variation of the semi-major axis and eccentricity of the fragments due to drag is computed with the King-Hele's formulation [5], according to the eccentricity value of each fragment.

2.3.   Spatial density function

Once the band has formed, the information on the single fragments can be translated into a continuous density function, which depends only on their Keplerian elements. The expression used for the spatial density function derives from Kessler [4]:

$$N(r, \beta) = n(r)f(\beta) \tag{1}$$

where $n(r)$ and $f(\beta)$ are the components of the spatial density accounting for the dependence on the radial distance r and on latitude β, defined as:

$$n(r) = \frac{1}{4\pi^2 r a^2} \frac{1}{\sqrt{e^2 - (\frac{r}{a} - 1)^2}} \tag{2}$$

$$f(\beta) = \frac{2}{\pi} \frac{1}{\sqrt{\cos^2 \beta - \cos^2 i}} \tag{3}$$

The expression for the spatial density is applied to each fragment at the band formation, then the total density function is found by summing each contribution.

2.4.   Continuum formulation

Once the initial spatial density is known at the band formation, the continuity equation is used to derive the evolution of the cloud spatial density in time, under the effect of atmospheric drag:

$$\frac{\partial n}{\partial t} + \nabla \cdot (n\mathbf{f}) = \dot{n}^+ - \dot{n}^- \tag{4}$$

where n is a generic density function, while $\nabla \cdot (n\mathbf{f})$ models atmospheric drag. Here, no discontinuous events are considered, hence $\dot{n}^+ - \dot{n}^- = 0$, as in [6]. To obtain the analytical solution, the assumptions of non-rotating atmosphere, spherical symmetry and quasi-circular orbits for the fragments in the band are made [6]. Introducing the parameter ϵ

$$\epsilon = \sqrt{\mu_E} \frac{c_d A}{M} \rho_{ref} \tag{5}$$

and the simplified expression for the radial velocity, putting $R_h = R_E + h_{ref}$

$$v_r = -\epsilon\sqrt{r}\exp(-\frac{r - Rh}{H}) \qquad (6)$$

The continuity equation can be elaborated into a first order Partial Differential Equation whose solution can be found with the method of characteristics. The final explicit expression for the density evolution can then be obtained:

$$n(r,t) = \frac{\Psi\left\{\exp[\frac{r-R_h}{H}] + (\epsilon\sqrt{R_h}/H)t\right\}}{-\epsilon r^{5/2}\exp[-\frac{r-R_h}{H}]}. \qquad (7)$$

The function Ψ is derived from the initial condition $n(r, t = 0)$ and from the characteristics at $t = 0$. To improve the accuracy of the method, the fragments are divided into an appropriate number of A/M bins [6], to account for their distribution in area-to-mass ratio. Then, the analytical solution is applied to each A/M bin separately, using an average value of ϵ. The corresponding partial densities are summed to obtain the global cloud density. The final solution is valid also for the evolution of the spatial density depending on the radial distance r and on latitude β, provided that Ψ is obtained with the expression of $N(r, \beta, t)$.

2.5.   A/M bins definition

To consider a distribution in A/M, three possible definitions for A/M bins have been tested:
- same fragment number: each bin contains the same number of fragments,
- logarithmically spaced: the bins have logarithmically spaced edges,
- constant $\Delta A/M$: the bins are spaced with a constant $\Delta A/M$.

The first two definitions were previously tested also by Letizia et al. in [6]. To evaluate the most accurate definition, two indicators have been considered to compare the results of the analytical method and of the numerical method (implemented with the same propagator used for the numerical propagation):
- err_{frag}, which is the relative error of the total number of fragments,
- err_{prof}, which is the absolute error between the two density profiles.

The analytical method is considered acceptable when err_{prof} and err_{frag} are, respectively, below 0.2 and 0.1. First, the debris cloud is propagated both with the analytical method using 10 A/M bins and with the numerical one, then the two

errors are computed at the end of the propagation to determine the best A/M bins definition. For the best definitions, the optimal number of A/M bins (between 1 and 15) providing the lowest errors is retrieved. For the whole analysis, 10 runs of the NASA breakup model have been used to obtain more reliable results.

3.   Collision probability

The second part of this work is devoted to study the consequences of fragmentation events by evaluating the collision probability for spacecraft crossing the debris cloud. In analogy with the kinetic theory of gases, the cumulative collision probability with a target is computed according to a Poisson distribution associated with gas kinetics, assuming that collisions between a target and the background debris population can be modelled as collisions among the molecules of an inert gas [6]. This hypothesis does not hold for the first phases of the cloud evolution, hence the collision probability is computed after band formation. The cumulative collision probability with the target can be computed as:

$$p_c(t) = 1 - \exp\left(-N_c(\Delta t)\right) \qquad (8)$$

where N_c is the cumulative number of collisions in the time interval Δt, which is estimated from the average impact rate $(\bar{\bar{\eta}})$ between the debris cloud and the target satellite:

$$\bar{\bar{\eta}} = \sigma_c N(r, \beta, t)\overline{v}_{rel} \qquad (9)$$

where $\overline{v}_{rel}$ is the average impact velocity and σ_c is the collisional cross-sectional area, equal to the target spacecraft area. The relative velocity can be found from geometrical considerations, however in this work the computation of the average impact velocity is corrected with respect to the previous implementation in [6], following the approach of Giudici et al. [2]. The averaging procedure is carried out with respect to the mean anomaly of the target $\overline{M}_T$ to account for all possible conjunctions between target and fragments while the target moves on its fixed orbit. In the general case of an elliptical orbit for the target, the impact rate can be computed with Eq. 10, with β_T target latitude and r_T target position. Then, the cumulative number of collisions in the time interval Δt can be found as:

$$N_c(t) = \bar{\bar{\eta}}\Delta t. \qquad (11)$$

$$\bar{\bar{\eta}} = \frac{\sigma_c}{2\pi} \int_0^{2\pi} N\left(r_T(f_T), \beta_T(f_T)\right) \frac{1}{2} \sum_{j=1}^{2} v_{rel}\left(\Delta\Omega_j(f_T)\right) \frac{d\overline{M}_T}{df_T} \, df_T \qquad (10)$$

4. Effect maps

The limited computational effort of the continuum approach allows to simulate numerous possible breakup scenarios. An analysis on the effects of breakups at several altitudes and inclinations is carried out on a set of target objects representing the active satellites in LEO. The effects of potential breakups are studied with the first formulation of the Environmental Consequences of Orbital Breakups (ECOB) index proposed by Letizia et al. [8]. This formulation of ECOB is a severity index since it only represents the risk posed by breakups to other objects in orbit without considering the likelihood of the fragmentation. To do this, a set of reference targets is defined. Then, the index is evaluated in a predefined grid in semi-major axis (25 km step) and inclination (5° step). A breakup is generated in each bin of the grid with the NASA Standard Breakup Model, the fragment cloud is propagated with the continuum approach for 15 years and the cumulative collision probability between fragments and the reference targets is computed. The final value of the index is computed as:

$$e = \frac{1}{A_{tot}} \sum_{j=1}^{N_t} p_c(t)_j A_j \qquad (12)$$

where e is also indicated as *effect* of collisions or explosions, A_{tot} is the total cross-section of all the representative targets, N_t is the number of targets, $p_c(t)_j$ the collision probability computed for each target j and A_j is the cumulative cross-section of the objects of the j-th bin.
The maps are generated first with a fixed time step Δt for the computation of the collision probability. Then, a novelty is introduced, computing the maps with a variable time step Δt to take into account the lifetime of debris clouds.

4.1. Lifetime of a debris cloud

Computing the effect maps with a variable Δt accounting for the lifetime of a debris cloud allows a more accurate representation of the effect of breakups occurring at low altitudes, where the lifetime is short. The lifetime of the cloud is computed as the average of the lifetimes of its fragments, which are evaluated with King-Hele's formulation [5] according to the eccentric-

ity value of each fragment. Then, the time step Δt is determined in accordance with the value of the lifetime. If the lifetime of the cloud exceeds 15 years, then Δt is set to 1 year, otherwise a proportion is used:

$$\Delta t(a) = \frac{\tau_L(a)}{15[\text{years}]} 365[\text{days}]. \qquad (13)$$

Moreover, an analysis is carried out to evaluate whether the propagation can be stopped earlier for debris clouds with a lifetime lower than 15 years. After the lifetime of the cloud, all the clouds with a variable Δt can be considered re-entered as at most 5% of the generated fragments are still in orbit, hence these clouds are propagated for a timespan equal to their lifetime.

5. Results

The main results concerning the propagation of a breakup are referred to a non-catastrophic collision between a 1500 kg spacecraft and a 2.665 kg projectile mass, with a relative velocity of 1 km/s. The characteristics of the breakup can be found in Table 1.

Table 1: Cosmos 1867 breakup characteristics.

| h_p [km]	h_a [km]	i_0 [deg]	M_e [kg]	N_F [-]
775	800	65	2.665	28136

5.1. A/M bins definition

For the evaluation of the best A/M bin definition, the reference breakup has been propagated with the continuum approach for 1000 days. The average errors over ten runs of the NASA Standard Breakup model are reported in Table 2.

Table 2: Average errors for the three bin definitions.

	$\overline{err}_{prof}$	$\overline{err}_{frag}$
Constant $\Delta A/M$	26.8%	7.5%
Logspaced	14.8%	6.95%
Same fragment n°	13.7%	7.03%

The two metrics essentially indicate an equivalence between logspaced bins and bins with the same number of fragments. As for bins with

a constant $\Delta A/M$, the two errors show that they lead to higher inaccuracies, despite guaranteeing the same accuracy for the description of the dynamics of each fragment. The other two definitions instead follow the distribution of the fragments, hence they are able to capture their lognormal A/M distribution. Therefore, these two definitions provide higher accuracy for fragments with smaller A/M ratios. The analysis of the optimal number of bins is carried out for logspaced bins and bins with the same number of fragments. The results in terms of the profile error and the fragment number error with respect to the number of bins are shown in Fig. 1a for logspaced bins and 1b for bins with the same number of fragments.
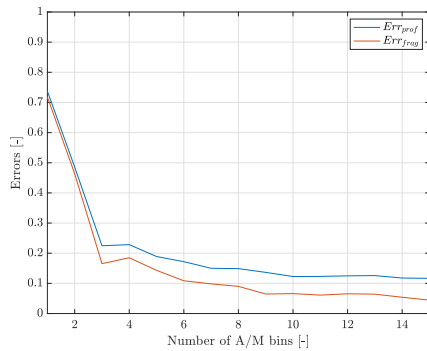
(a) Errors for logspaced bins.
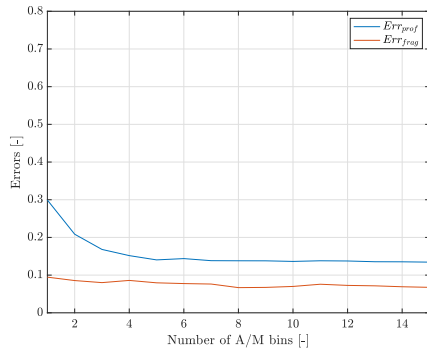
(b) Errors for bins with the same number of fragments.

Figure 1: Errors for logspaced bins (a) and for bins with the same number of elements (b).

For logspaced bins and for the profile error of bins with the same number of objects, using a low number of bins entails a high error, while at around 10 bins the error reaches a plateau, hence 10 bins should be enough to guarantee an accurate representation. The error on the number of fragments for bins with the same number of objects instead does not exhibit a well defined

behaviour. The dependence on the altitude of the breakup is studied and the result is shown in Fig. 2.
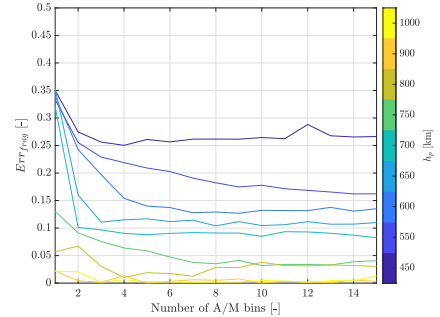

Figure 2: Fragment number error for bins with the same number of fragments with respect to the altitude of the breakup.

The plot shows that the higher the altitude of the breakup, the lower the error. It is safe to assume that also for the bins with the same number of objects 10 bins should be enough to have an accurate description. The high errors for the breakups occurring at low altitudes are caused by the extension of the continuum approach below the altitude for which it has been validated.

5.2.   Fragmentation event

Here, the results for the non-catastrophic collision taken as reference scenario are presented. A typical diagram used to represent the distribution of the fragments generated in a breakup is the Gabbard diagram. Its alternative representation after the fragmentation and at band formation is represented in Fig. 3a and 3b.
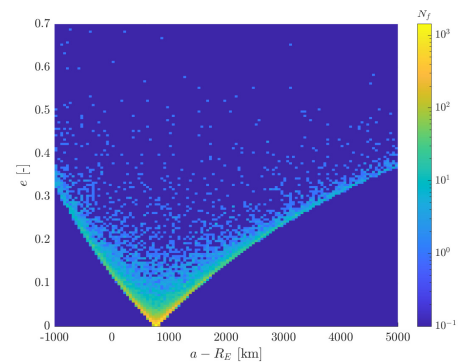
(a) At fragmentation.
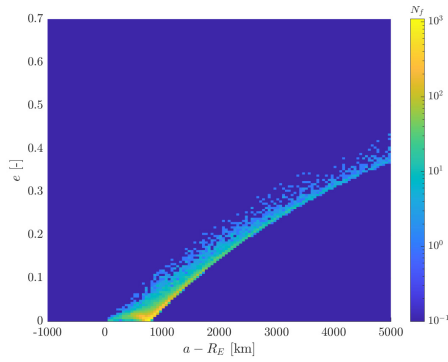
(b) At band formation.

Figure 3: Gabbard diagram at fragmentation (a) and at band formation (b).

Fig. 3a shows a typical V-shaped distribution centred at the altitude and eccentricity of the breakup. The effect of atmospheric drag can be seen in the reduction in apogee over time, leading to the circularisation of the orbits of fragments with low semi-major axis and the disappearance of the left leg of the diagram due to fragments re-entering. The continuum approach is applied at band formation, propagating the debris cloud for 1000 days. The evolution of the cloud spatial density for each A/M bin is presented in Fig. 4.
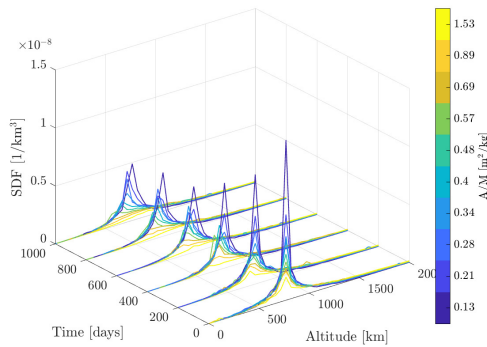
Figure 4: Evolution of the spatial density of the debris cloud for 1000 days.
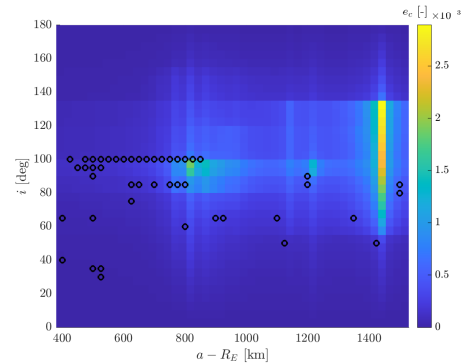
5.3. Effect maps

The effect maps for catastrophic collisions, non-catastrophic collisions and explosions have been generated, considering a reference mass of 1000 kg. This is motivated by the correlation between the value of the fragmenting mass and of the index [9]. Indeed, once the effect maps for a fixed mass have been obtained, it is sufficient to rescale them to derive the results for a different fragmenting mass. Only the effect maps concerning catastrophic collisions are shown in this
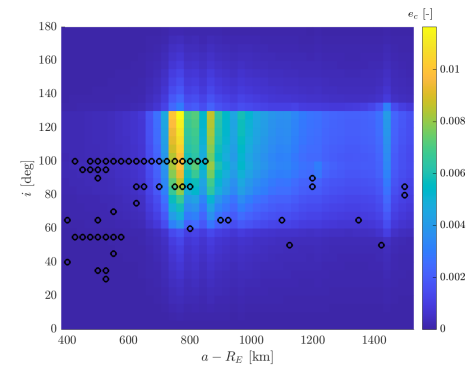
section. The maps are computed for representative targets of 2017, 2023 without the Starlink constellation and 2023 with the Starlink constellation. The results of the maps computed with a fixed Δt can be found in Fig. 5a, 5b, 5c.
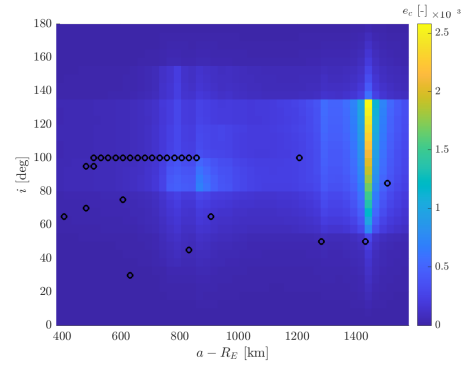
(a) 2017.

(b) 2023.

(c) 2023 with Starlink.

Figure 5: Effect maps of catastrophic collisions with targets of 2017 (a), 2023 (b) and 2023 with Starlink constellation (c), with a fixed Δt. Fragments lower size limit: 1 cm.

The 2023 map without Starlink (Fig. 5b) is used as reference for comparison with the maps obtained with the THEMIS software developed by Politecnico di Milano [1]. The map shows the same order of magnitude in the effect and the same concentration of the effect as the THEMIS one in the altitude region around 800 km, with

6

the peak at 90°, and slightly above 1400 km, with the peak at 130°. The differences in the maps may be due to the fact that the maps in this work are obtained with the extension of the analytical approach beyond the regions for which it has been validated.

The increase of representative targets in 2023 with respect to 2017 has caused a growth in the effect of catastrophic collisions, especially around 800 km of altitude. With the addition of Starlink, the effect increases of up to one order of magnitude and the most significant repercussions of Starlink can be found between 800 and 1000 km. This is due to the fact that the breakups occurring at lower altitudes re-enter the atmosphere faster than those at higher altitudes, whose fragments decay throughout the 15 years of propagation under the effect of drag, therefore running into Starlink and increasing the collision probability. Moreover, the peak of the effect can be seen at around 125°, which is to be expected since the majority of Starlink representative targets has an inclination of 55°.

The same maps have been computed with a variable Δt. The maps for the reference targets of 2017 and 2023 without Starlink do not exhibit significant differences with respect to the maps computed with a fixed Δt, however the map including Starlink presents distinct changes as shown in Fig. 6.
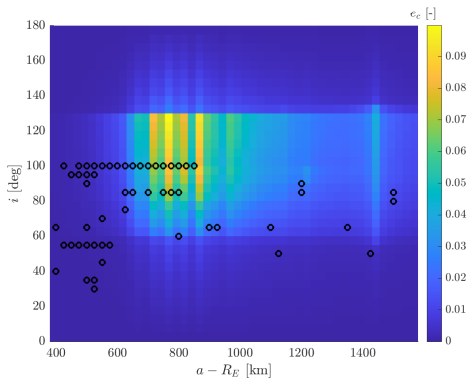

Figure 6: Effect map of catastrophic collisions with targets of 2023 with Starlink constellation, with a variable Δt. Fragments lower size limit: 1 cm.

Using a variable Δt leads to a higher absolute value of the effect. Moreover, higher values of the effect can be found at lower altitudes with respect to Fig. 5c, reaching almost 600 km. It is therefore clear that using a variable Δt gives a better representation of the consequences of fragmentation events at low altitudes.

6.   Conclusions

The aim of this work was the development of a continuum approach to study debris clouds and to assess the collision probability of target spacecraft with the fragments. The long-term evolution of debris clouds has been tackled through the continuity equation, monitoring the changes of spatial density in time. To increase the accuracy of the method, it has been found that subdividing the fragments into bins according to their area-to-mass ratio either by using the same number of fragments in each bin or logarithmically spaced bins provides the best results. This approach was able to provide accurate results in reduced computational time. The application of the method is the generation of effect maps, to evaluate the severity of breakups occurring at several altitudes and inclinations in the LEO region. The resulting maps show that the severity of breakups increases with the growing number of operational satellites in time. This is particularly evident when constellations such as Starlink are included in the target sets, making the consequences of breakups more severe. Moreover, using a variable Δt related to the lifetime of the debris clouds provides more accurate insights into the effects of breakups occurring at low altitudes.

7.   Acknowledgements

References

[1] Camilla Colombo, Andrea Muciaccia, Lorenzo Giudici, Juan Luis Gonzalo, Alessandro Masat, Mirko Trisolini,

Borja Del Campo, Francesca Letizia, and Stijn Lemmens. Tracking the health of the space debris environment with themis. *Aerospace Europe Conference 2023 – 10th EUCASS – 9th CEAS*, 2023.

[2] Lorenzo Giudici, Juan Luis Gonzalo, and Camilla Colombo. Density-based in-orbit collision risk model extension to any impact geometry, 2023. arXiv:2309.03562.

[3] N. L. Johnson, P. H. Krisko, J. C. Liou, and P. D. Anz-Meador. Nasa's new breakup model of evolve 4.0. *Advances in Space Research*, 28, 2001.

[4] Donald J. Kessler. Derivation of the collision probability between orbiting objects: the lifetimes of jupiter's outer moons. *Icarus*, 48, 1981.

[5] D. G. King-Hele. *Theory of Satellite Orbits in an Atmosphere.* Butterworths, 1964.

[6] Francesca Letizia. *Space debris cloud evolution in Low Earth Orbit.* PhD thesis, University of Southampton, Faculty of Engineering and the Environment, 2016.

[7] Francesca Letizia, Camilla Colombo, and Hugh G. Lewis. Collision probability due to space debris clouds through a continuum approach. *Journal of Guidance, Control, and Dynamics*, 39, 2016.

[8] Francesca Letizia, Camilla Colombo, Hugh G. Lewis, and Holger Krag. Assessment of breakup severity on operational satellites. *Advances in Space Research*, 58, 2016.

[9] Francesca Letizia, Camilla Colombo, Hugh G. Lewis, and Holger Krag. Development of a debris index. *Astrophysics and Space Science Proceedings*, 52, 2018.

[10] D. McKnight. A phased approach to collision hazard analysis. *Advances in Space Research*, 10, 1990.